IJCRT.ORG ISSN : 2320-2882

INTERNATIONAL JOURNAL OF CREATIVE RESEARCH THOUGHTS (IJCRT)

An International Open Access, Peer-reviewed, Refereed Journal

Thermal Analysis Of Triangular Porous Fin With Power Law Dependent Thermal Parameters And Magnetic Effects

Bipattaran Raj[1], Pranab Kanti Roy[2]

[1]Department of Mathematics, Seacom Skills University, Kendradangal, Birbhum-731236, West Bengal, India

[2]Department of Mechanical Engineering, Seacom Skills University, Kendradangal, Birbhum-731236, West Bengal, India

Abstract

This study presents a closed-form solution for a triangular porous fin, incorporating factors such as power law-dependent heat transfer coefficient, internal heat generation, surface emissivity, and external magnetic and electric fields. Darcy's model is used to simulate flow within the fin under insulated boundary conditions. The governing equation is solved using the Modified Adomian Decomposition Method (MADM), with results compared to the Finite Difference Method (FDM) for validation. The analysis shows that the fin temperature increases with higher power law parameters, and both the Hartmann number (magnetic field effect) and porosity improve fin efficiency.

Keywords: variable area; porosity; magnetic effect; modified differential operator

Nomenclature

k	Thermal conductivity, $\frac{W}{m.K}$
$T(x)$	Temperature function of fin length, K
P_x	Perimeter at location x, m
T_b	Dimensional temperature at the base, K
T_a	Temperature at ambient condition, K

$q(T)$ Internal heat generation power function of (T, T_a, T_b), $\frac{W}{m^3}$

$h(T)$ Heat transfer co-efficient, $\frac{W}{m^2.K}$

n, B, ε_G Power exponent Heat transfer co-efficient, Surface emissivity, Internal heat generation

R_a Modified form of Rayleigh number, $\frac{gKb(T_b - T_a)L}{agk_R y}$,

R_d Radiation-conduction parameter, $\frac{4\sigma T_a^3}{3k_{eff}\beta_R}$

R_2 Surface ambient-radiation parameter, $R_2 = \frac{4\sigma\varepsilon_s T_a^3 L}{k_{eff}\psi}$

H_a Hartmann number, $\frac{\sigma_m B_0^2 V^2 L^2}{k_{eff}(T_b - T_a)}$

Z_0 Fin parameter, $\sqrt{\frac{h_b L^2}{k_{eff} y_b}}$

G Heat generation number, $\frac{q_0 L^2}{k_{eff}(T_b - T_a)}$

k_R Thermal conductivity ratio, $\frac{k_{eff}}{k_f}$

x Axial co-ordinate measured from fin tip, m

y Vertical co-ordinate measured from fin tip, m

A_x Cross-section at the location x, m^2

X Dimensionless co-ordinate measured from fin tip, $\frac{x}{L}$

J_c Conduction current density, $\frac{A}{m}$

E External electric field

B_0 Magnetic Field, *Tesla*

V_w Darchy velocity, $\frac{m}{s}$

V Macroscopic velocity of fluid due to electric and magnetic field, $\frac{m}{s}$

C_p Specific Heat, $\frac{J}{kg.K}$

b Width, m

t_b Thickness at the base, m

E Electrical field, $\frac{V}{m}$

$\varepsilon(T)$ Surface emissivity of power function of (T, T_a, T_b),

ψ Half fin thickness measured at the base to length ratio, $\frac{y_b}{L}$

λ Half fin thickness measured at the base to width in dimensionless form, $\frac{y_b}{b}$

φ Parameter denote porosity

θ Temperature in dimensionless form, $\frac{T-T_a}{T_b-T_a}$

ε_s Emissivity parameter of surface w.r.t. atmosphere

σ Stephen-Boltzmann constant, $\frac{W}{m^2.K^4}$

γ Kinematic viscosity, $\frac{m^2}{s}$

α Thermal diffusivity, $\frac{k_f}{\rho C_p}$

ρ Fluid density, $\frac{kg}{m^3}$

β Thermal expansion co-efficient, $\frac{1}{K}$

ω $\frac{1}{2\lambda}$

σ_m Electrical conductivity, $\frac{A}{m}$

β_R Mean absorption co-efficient of Rossland

1. Introduction

Extended surfaces are essential components in thermal engineering, used to enhance heat transfer from a solid surface to the surrounding environment. The design of fins varies based on the specific application, taking into account factors like material efficiency, production costs, and ease of fabrication. Among the different shapes, rectangular fins are the most common due to their simplicity and broad range of applications, such as in electronics, automotive industries, and more [1-3]. This study explores fin profiles like triangular, convex/concave, and exponential, focusing on applications where lightweight and material efficiency are keys, such as in space technology. Triangular fins are preferred for their reduced volume and ease of manufacturing. Kraus [4] provides a detailed review of fin designs.

In the past two decades, research on porous fins has increased due to their ability to enhance heat dissipation by increasing surface area through interconnected voids. Early studies focused on how different parameters affect the thermal performance of porous surfaces [5, 6]. Kiwan and Al-Nimr [7] studied porous fins for improved heat transfer under different conditions. Kiwan [8] explored natural convection in porous fins, while Gorla and Bakier [9] showed that porous fins outperform solid fins in heat transfer. Kundu and Bhanja [10] optimized porous fins using various models, and in [11], they found that Constructal T-shape porous fins offer better heat transfer when using the appropriate porous medium.

Various methods, including the Differential Transformation Method (DTM), are used to solve non-linear problems in porous fins with singularities. Moradi et al. [12] applied DTM to analyze triangular porous fins, achieving good agreement with the Runge-Kutta method. Hatami et al. [13] used DTM, Collocation Method (CM), and Least Square Method (LSM) to solve non-singular energy equations for rectangular fins made of Si3N4 and Al. Oguntala et al. [14] applied the Daftardar-Gejiji and Jafari Method (DJM) to solve the non-singular energy equation for a constant cross-section porous fin, with results matching the Runge-Kutta method. Roy et al. [15] used the Adomian Decomposition Method (ADM) for non-linear rectangular fins and the Modified Adomian Decomposition Method (MADM) for singular convex and triangular fins, achieving good agreement with exact solutions. They applied similar methods for heat transfer analysis in solar collectors with power law-dependent thermal properties [15, 16].

Many studies have focused on fins with temperature-dependent properties, using power law for heat transfer coefficients and linear or polynomial relations for other parameters. Mosayebidorcheh et al. [17] and Moitsheki et al. [18] applied power law to thermal conductivity and heat transfer coefficients in rectangular fins, extending it to variable cross-sections [19]. Porous fins, with their interconnected voids, benefit from electric and magnetic fields, which enhance heat transfer by ionizing gas particles. Studies by Sobamowo [20], Das and Kundu [21], Hoshyar et al. [22], and Patel and Meher [23] examined the impact of these fields on porous fins, while Gireesha et al. [24] and Madhura et al. [25] investigated porous fins with varying thermal properties and conductivity. Das and Kundu [26] also studied heat transfer in longitudinal porous fins for electronic cooling.

The current research addresses a gap in the literature by studying the multiple variations of thermo-physical parameters in porous triangular fins. It aims to unify these variations into a single mathematical framework to better predict heat transfer, while also exploring how an external magnetic field enhances the heat transfer rate.

2. Methodology

This study aims to find closed-form solutions for a triangular porous fin with power law-dependent thermal properties, using Darcy's equation for fluid flow influenced by electric and magnetic fields. The singular non-linear energy equation is solved using the Modified Adomian Decomposition Method (MADM), with results compared to the Finite Difference Method (FDM).

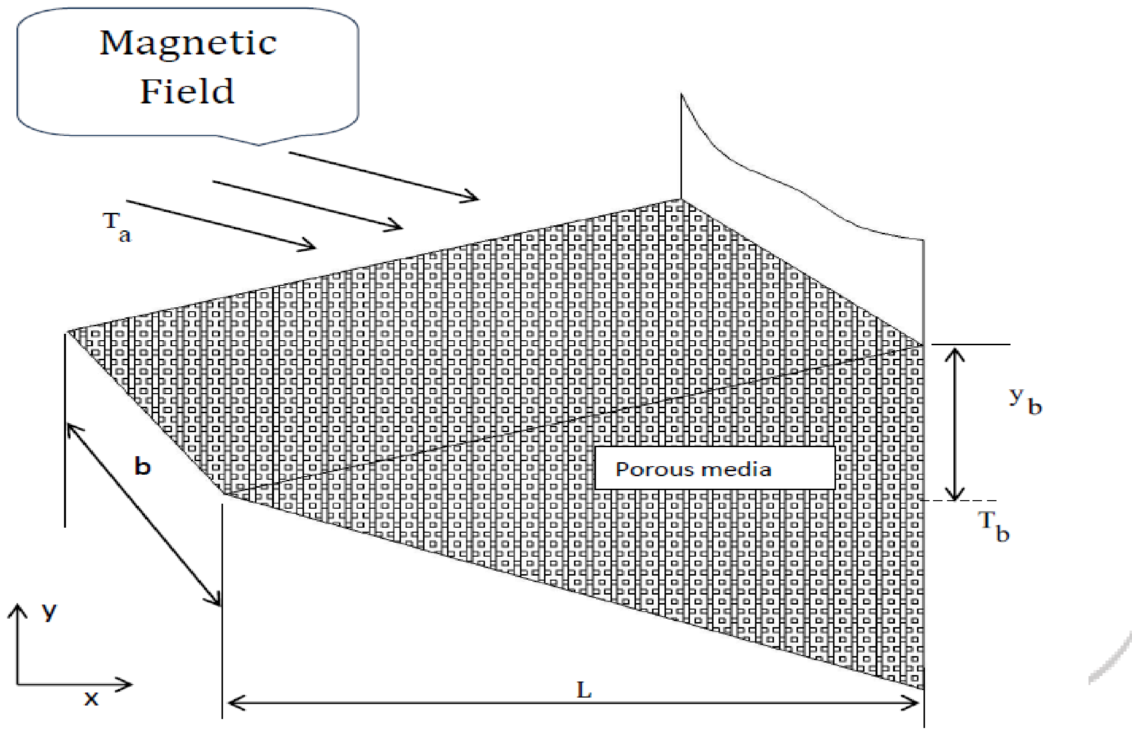

Figure1 (a) A crucial aspect of the three-dimensional porous fin with a triangle cross-section

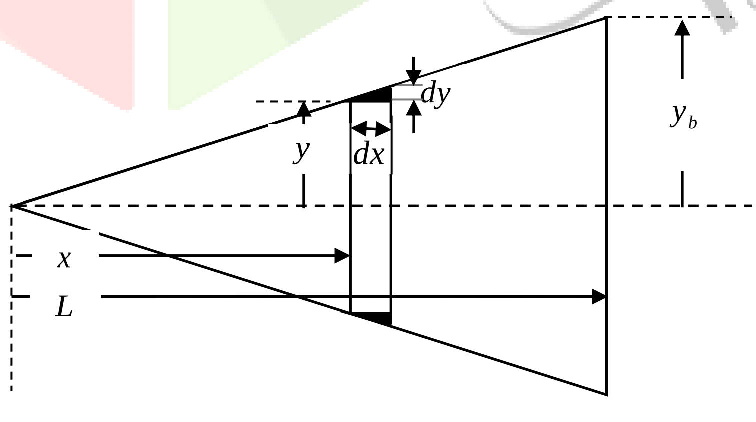

Figure1 (b) Triangular porous fin in vertical plane with physical coordinates

3. Mathematical Formulation of the physical problem

Figure 1(a) shows a triangular cross-section porous fin with its base attached to a constant-temperature plate. Assumptions include an isotropic, homogeneous medium with no phase change, local thermal equilibrium between fluid and porous medium, a steady one-dimensional model, Darcy's law for fluid flow, and a vertically applied uniform magnetic field with temperature varying only in the x-direction.

The energy equation for the differential element at a location x from the tip of the porous fin as

$$\frac{dq_x}{dx}dx + q(t)A_x dx = h(t)P_x(1-\phi)(T-T_a) + \dot{m}C_m(T-T_a) + \sigma\varepsilon(t)P_x dx\left(T^4 - \frac{\alpha}{\varepsilon_s}T_a{}^4\right) + \frac{J_c \times J_c}{\sigma_m}dx \qquad (1)$$

Where A_x is area P_x perimeter at the location x. For solving the equation (1) two boundary conditions are required as follows

$$At\ tip: \quad T(x)\big]_{x=0} = 0 \qquad 2(a)$$

$$At\ base: \quad T(x)\big]_{X=L} = T_b \qquad 2(b)$$

The power law variations of thermophysical parameters are applied as follows,

$$h(T) = h_b\left(\frac{T-T_a}{T_b-T_a}\right)^n \qquad 3(a)$$

$$\varepsilon(T) = \varepsilon_s\left(\frac{T-T_a}{T_b-T_a}\right)^B \qquad 3(b)$$

$$q(T) = q_0\left(\frac{T-T_a}{T_b-T_a}\right)^{\varepsilon_G} \qquad 3(c)$$

Figure 1(b) illustrates the geometrical relationship of the fin in the vertical plane using the similarity law.

$\frac{dy}{dx} = \frac{y_b}{L}$ and $\frac{y}{x} = \frac{y_b}{L}$

Since vertical distance y is linear function of x therefore cross-sectional area A_x and perimeter P_x for the triangular fin from tip to base is calculated as follows

$$A_x = 2\times\frac{y}{2}b = \left(\frac{x}{L}\right)y_b b \qquad (4)$$

$$P_x = (2y+b)\sqrt{1+\left(\frac{dy}{dx}\right)^2} \qquad (5)$$

The mass flow rate $\dot{m}$ and Darcy's velocity related by the relation $\dot{m} = \rho V_W(2y+b)\sqrt{1+\left(\frac{dy}{dx}\right)^2}dx$. The cross product of current density produces the magnetic field in the porous media and it can be related as follows

$$\frac{J_c \times J_c}{\sigma_m} = \sigma_m B_0^{\,2} V^2 \left(\frac{x}{L} y_b\right)\left(\frac{T - T_a}{T_b - T_a}\right) \qquad (6)$$

The conduction-radiation energy transfer rate from fin's base is given below

$$q = q_{cond.} + q_{rad.} = -k_{eff}\left(\frac{y_b x}{L}\right)\frac{dT}{dx} - \frac{4\sigma}{3\beta_R}\left(\frac{y_b x}{L}\right)\frac{dT^4}{dx} \qquad (7)$$

Using $T^4 \approx 4T_a^{\,3} T - 3T_a^{\,4}$ and employing the non dimensional terms, the energy equation (5) can be rewritten as follows,

$$\frac{d}{dX}\left(X\frac{d\theta}{dX}\right) + \frac{G}{(1+4R_d)} X\theta^{\varepsilon_G} = 2\lambda(X+\omega)\sqrt{1+\psi^2}\,\frac{Z_0^{\,2}(1-\phi)}{(1+4R_d)}\theta^{n+1} + 2\lambda(X+\omega)\sqrt{1+\psi^2}\,\frac{R_a}{(1+4R_d)}\theta^2$$
$$+ 2\lambda(X+\omega)\sqrt{1+\psi^2}\,\frac{R_2}{(1+4R_d)} + X\frac{H_a}{(1+4R_d)} \qquad (8)$$

The following boundary conditions are required to solve the above equations

$$\text{At tip}: \quad \theta(X)\big]_{X=0} = 0 \qquad (9a)$$
$$\text{At base}: \quad \theta(X)\big]_{X=1} = 1 \qquad (9b)$$

$$\frac{d^2\theta}{dX^2} + \frac{1}{X}\frac{d\theta}{dX} = -\frac{G}{(1+4R_d)}\theta^{\varepsilon_G} + \frac{2\lambda\sqrt{1+\psi^2}}{(1+4R_d)} Z_0^{\,2}(1-\phi)\theta^{n+1} + \frac{2\lambda\sqrt{1+\psi^2}}{(1+4R_d)}\omega Z_0^{\,2}(1-\phi)\left(\frac{\theta^{n+1}}{X}\right)$$
$$+ \frac{2\lambda\sqrt{1+\psi^2}}{(1+4R_d)} R_a\theta^2 + \frac{2\lambda\sqrt{1+\psi^2}}{(1+4R_d)}\omega R_a\left(\frac{\theta^2}{X}\right) + \frac{2\lambda\sqrt{1+\psi^2}}{(1+R_d)} R_2\theta^{B+1} + \frac{2\lambda\sqrt{1+\psi^2}}{(1+4R_d)}\omega R_2\left(\frac{\theta^{B+1}}{X}\right)$$
$$+ \frac{H_a}{(1+4R_d)}\theta \qquad (10)$$

The above equation (10) will be solved by modified ADM. According to the MADM the LHS of the equation (10) will form the modified differential operator as follows

$L_X = X^{-1}\frac{d}{dX} X \frac{d}{dX}(\bullet)$ and it is invertible and therefore its inverse operator can be written as follows

$$L_X^{\,-1} = \int_0^X X^{-1}\int_0^X X(\bullet)\,dX\,dX$$

The equation (10) can be written in operator form

$$L_X\theta = -\frac{G}{(1+4R_d)}(NA) + \frac{2\lambda\sqrt{1+\psi^2}}{(1+4R_d)} Z_0^{\,2}(1-\phi)(NB_1) + \frac{2\lambda\sqrt{1+\psi^2}}{(1+4R_d)}\omega Z_0^{\,2}(1-\phi)\left(\frac{NB_2}{X}\right) +$$
$$\frac{2\lambda\sqrt{1+\psi^2}}{(1+4R_d)} R_a(NC_1) + \frac{2\lambda\sqrt{1+\psi^2}}{(1+4R_d)}\omega R_a\left(\frac{NC_2}{X}\right) + \frac{2\lambda\sqrt{1+\psi^2}}{(1+4R_d)} R_2(ND_1) + \frac{2\lambda\sqrt{1+\psi^2}}{(1+4R_d)}\omega R_2\left(\frac{ND_2}{X}\right)$$
$$+ \frac{H_a}{(1+4R_d)}\theta \qquad (11)$$

The non-linear terms are expanded in Adomian polynomials in the manner given below

$$NA=\theta^{\varepsilon_G}=\sum_0^m A_m;$$

$$A_0=\theta_0^{\varepsilon_G};$$

$$A_1=\varepsilon_G\theta_0^{\varepsilon-1}\theta_1;$$

…

$$NB1=NB2=\theta^{n+1}=\sum_0^m B_m;$$

$$B_0=\theta_0^{n+1};$$

$$B_1=(n+1)\theta_0^{n}\theta_1;$$

…

$$NC1=NC2=\theta^2=\sum_0^m C_m;$$

$$C_0=\theta_0^{2};$$

$$C_1=2\theta_0\theta_1;$$

…

$$ND1=ND2=\theta^{B+1}=\sum_0^m D_m;$$

$$D_0=\theta_0^{B+1};$$

$$D_1=(B+1)\theta_0^{B}\theta_1;$$

…

Multiplying by the inverse operator on both sides of the equation (11) and expanding the RHS in Maclaurin series expansion

$$\theta=\theta(0)+X\frac{d\theta(0)}{dX}-\frac{G}{(1+4R_d)}L_X^{-1}\left(\sum_0^\alpha A_m\right)+\frac{2\lambda\sqrt{1+\psi^2}}{(1+4R_d)}Z_0^2(1-\phi)L_X^{-1}\left(\sum_0^\alpha B_m\right)$$
$$+\frac{2\lambda\sqrt{1+\psi^2}}{(1+4R_d)}\omega Z_0^2(1-\phi)L_X^{-1}\left(\frac{\sum_0^\alpha B_m}{X}\right)+\frac{2\lambda\sqrt{1+\psi^2}}{(1+4R_d)}R_aL_X^{-1}\left(\sum_0^\alpha C_m\right)+$$
$$\frac{2\lambda\sqrt{1+\psi^2}}{(1+4R_d)}\omega R_aL_X^{-1}\left(\frac{\sum_0^\alpha C_m}{X}\right)+\frac{2\lambda\sqrt{1+\psi^2}}{(1+4R_d)}R_2L_X^{-1}\left(\sum_0^\alpha D_m\right)+\frac{2\lambda\sqrt{1+\psi^2}}{(1+4R_d)}\omega R_2L_X^{-1}\left(\frac{\sum_0^\alpha D_m}{X}\right)$$
$$+\frac{H_a}{(1+4R_d)}L_X^{-1}\left(\sum_0^\alpha\theta_m\right) \qquad (12)$$

The first component θ_0 is calculated as below

$$\theta_0 = \theta(0) + X\frac{d\theta(0)}{dX} = C$$

Using the recursive relation next higher order terms are computed as follows

$$\theta_{m+1} = -\frac{G}{(1+4R_d)}L_X^{-1}\left(\sum_0^{\alpha} A_m\right) + \frac{2\lambda\sqrt{1+\psi^2}}{(1+4R_d)}Z_0^2(1-\phi)L_X^{-1}\left(\sum_0^{\alpha} B_m\right) + \frac{2\lambda\sqrt{1+\psi^2}}{(1+4R_d)}\omega Z_0^2(1-\phi)L_X^{-1}\left(\frac{\sum_0^{\alpha} B_m}{X}\right) + \frac{2\lambda\sqrt{1+\psi^2}}{(1+4R_d)}R_a L_X^{-1}\left(\sum_0^{\alpha} C_m\right) + \frac{2\lambda\sqrt{1+\psi^2}}{(1+4R_d)}\omega R_a L_X^{-1}\left(\frac{\sum_0^{\alpha} C_m}{X}\right) + \frac{2\lambda\sqrt{1+\psi^2}}{(1+4R_d)}R_2 L_X^{-1}\left(\sum_0^{\alpha} D_m\right) + \frac{2\lambda\sqrt{1+\psi^2}}{(1+4R_d)}\omega R_2 L_X^{-1}\left(\frac{\sum_0^{\alpha} D_m}{X}\right) + \frac{H_a}{(1+4R_d)}L_X^{-1}\left(\sum_0^{\alpha}\theta_m\right), m \ge 0 \quad (13)$$

The second component is calculated as follows

$$\theta_1 = -\frac{G}{(1+4R_d)}L_X^{-1}(A_0) + \frac{2\lambda\sqrt{1+\psi^2}}{(1+4R_d)}Z_0^2(1-\phi)L_X^{-1}(B_0) + \frac{2\lambda\sqrt{1+\psi^2}}{(1+4R_d)}\omega Z_0^2(1-\phi)L_X^{-1}\left(\frac{B_0}{X}\right) + \frac{2\lambda\sqrt{1+\psi^2}}{(1+4R_d)}R_a L_X^{-1}(C_0) + \frac{2\lambda\sqrt{1+\psi^2}}{(1+4R_d)}\omega R_a L_X^{-1}\left(\frac{C_0}{X}\right) + \frac{2\lambda\sqrt{1+\psi^2}}{(1+4R_d)}R_2 L_X^{-1}(D_0) + \frac{2\lambda\sqrt{1+\psi^2}}{(1+4R_d)}\omega R_2 L_X^{-1}\left(\frac{D_0}{X}\right) + \frac{H_a}{(1+4R_d)}L_X^{-1}(\theta_0) \quad (14)$$

The third component is calculated as follows

$$\theta_2 = -\frac{G}{(1+4R_d)}L_X^{-1}(A_1) + \frac{2\lambda\sqrt{1+\psi^2}}{(1+4R_d)}Z_0^2(1-\phi)L_X^{-1}(B_1) + \frac{2\lambda\sqrt{1+\psi^2}}{(1+4R_d)}\omega Z_0^2(1-\phi)L_X^{-1}\left(\frac{B_1}{X}\right) + \frac{2\lambda\sqrt{1+\psi^2}}{(1+4R_d)}R_a L_X^{-1}(C_1) + \frac{2\lambda\sqrt{1+\psi^2}}{(1+4R_d)}\omega R_a L_X^{-1}\left(\frac{C_1}{X}\right) + \frac{2\lambda\sqrt{1+\psi^2}}{(1+4R_d)}R_2 L_X^{-1}(D_1) + \frac{2\lambda\sqrt{1+\psi^2}}{(1+4R_d)}\omega R_2 L_X^{-1}\left(\frac{D_1}{X}\right) + \frac{H_a}{(1+4R_d)}L_X^{-1}(\theta_1) \quad (15)$$

Therefore, final solution is the summation of three components.

$$\theta = \sum_0^m \theta_m = \theta_0 + \theta_1 + \theta_2 \cdots \quad (16)$$

The actual rate of heat transfer of the porous fin from base to tip can be determined using Fourier's law of heat conduction

$$q_{actual} = \frac{k_{eff}\, y_b b(T_b - T_a)(1+4R_d)}{L} X \frac{d\theta}{dX}\Big]_{X=0} \tag{17}$$

The maximum heat transfer is possible if its area and perimeter are calculated at base.

$$q_{\max} = -q_0\left[y_b bL\right] + h_b(1-\phi)(T_b - T_a)\left[bL\sqrt{1+\psi^2} + y_b L\right] + \frac{\rho g C_p K\beta (T_b - T_a)^2}{\gamma}\left[bL\sqrt{1+\psi^2} + y_b L\right] + 4\sigma\varepsilon_s T_a^{\,3}(T_b - T_a)\left[bL\sqrt{1+\psi^2} + y_b L\right] + \sigma_m B_0^{\,2} V^2 (y_b bL) \tag{18}$$

The efficiency (η) of the triangular porous fin can be obtained by the expression

$$\eta = \frac{q_{actual}}{q_{\max}} \frac{X \frac{d\theta}{dX}\Big|_{X=0}}{-\frac{G}{(1+4R_d)} + \frac{Z_0^{\,2}(1-\phi)\left(\sqrt{1+\psi^2}+\lambda\right)}{(1+4R_d)} + \frac{R_a\left(\sqrt{1+\psi^2}+\lambda\right)}{(1+4R_d)} + \frac{R_2\left(\sqrt{1+\psi^2}+\lambda\right)}{(1+4R_d)} + \frac{H_a}{(1+4R_d)}} \tag{19}$$

4. Results and discussion

This study examines the effects of power law index for heat transfer coefficient, internal heat generation, and surface emissivity in a triangular porous fin under external electric and magnetic fields. The energy equation, which involves non-linearity and singularity, is solved using the Modified Adomian Decomposition Method (MADM). In order to validate the present results, the governing equations are converted into only singular value equations by putting, $G = \varepsilon_G = n = B = R_d = H_a = R_a = R_2 = \omega = \psi = 0, \lambda = 1, Z_0 = 1.5$ and as shown below,

$$X\frac{d^2\theta}{dX^2} + \frac{d\theta}{dX} = (X + \frac{1}{2})Z_0^{\,2}\theta \tag{20}$$

The above equation is solved numerically using FDM and both the results of FDM and MADM are plotted for their comparison as shown in **Figure 2.**

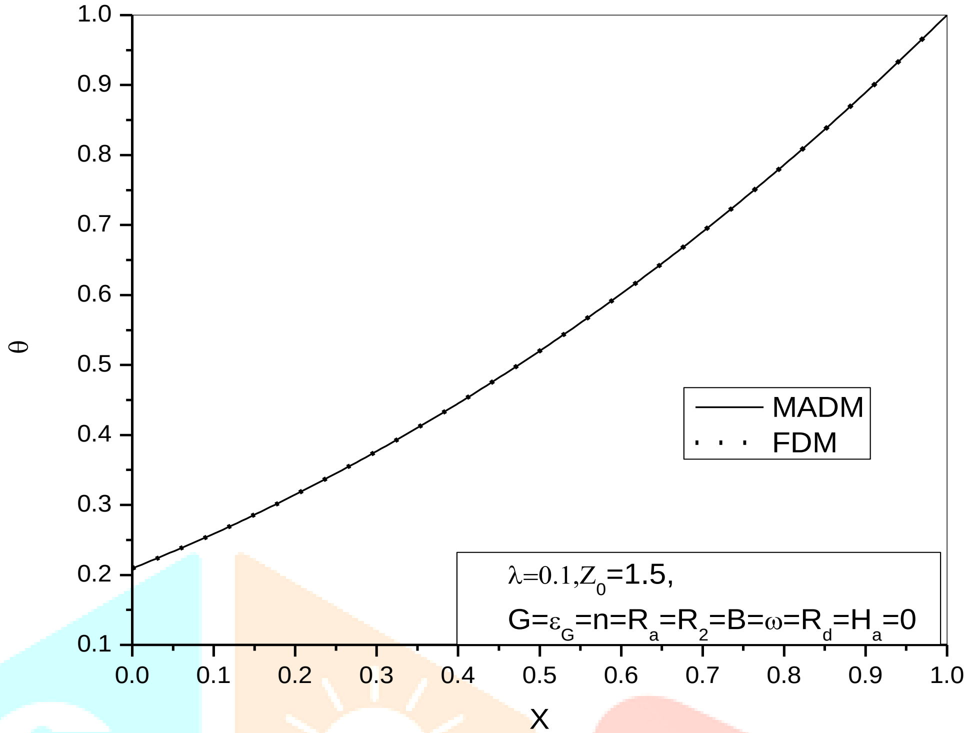

Figure 2. Comparison of MADM and FDM for the values of Z_0.

Table 1 Range of values for physical and thermal parameters

G	$\varepsilon_G = n = B$	R_a	R_2	R_d	H_a	λ	Z_0
0.001	0-0.5	0.001-0.1	0.001	0.001-0.1	0-0.2	0.01-1	1.1-2

The energy equation comprises twelve thermo-physical parameters, and a higher value of these parameters results in an increase in the absolute error at the fin tip, potentially leading to an unreliable solution for the problem. In each figure, the power law values are varied together while maintaining the same levels. The values for heat generation number and surface ambient radiation parameters are kept constant at low levels, and the other parameter ranges for the current problem are as presented in **Table 1. Figure 3** exhibits of the effects of combine power index of h, ε and q, on the temperature curves for the specific values of 0, 0.25 and 0.5 and all the three values are separately exhibited at R_a at 0.001 and 0.1 respectively.

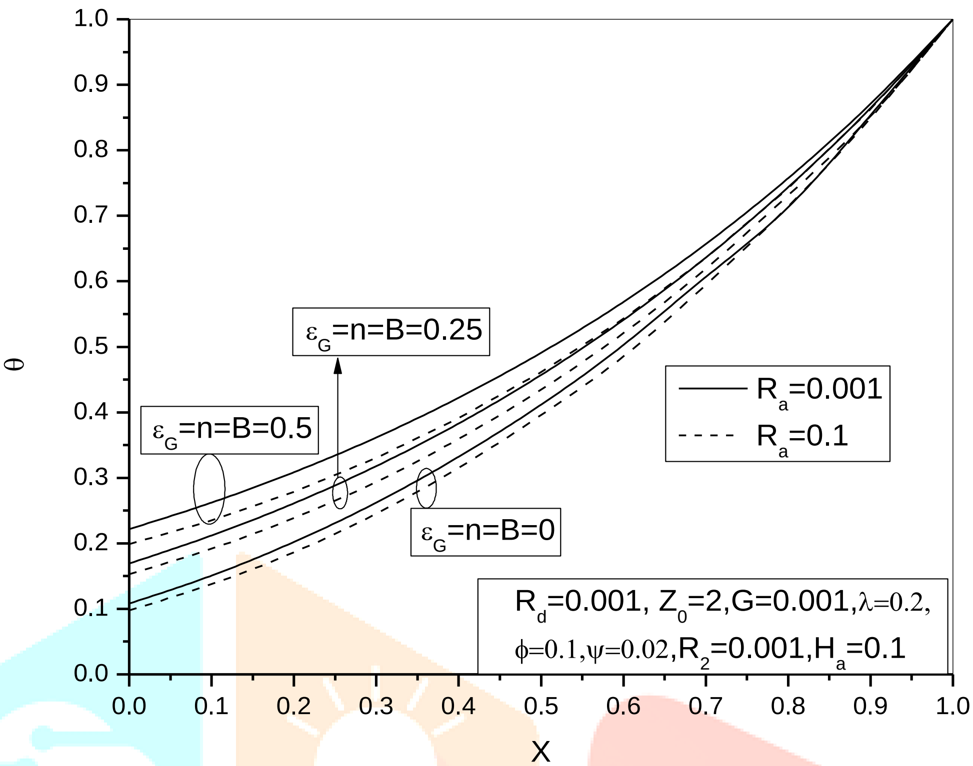

Figure 3. Effects of combine power index of *h*, ε and *q* on the temperature curves for the specific values of 0, 0.25 and 0.5 for the values of R_a at 0.001 and 0.1 respectively.

The bottom solid and dashed lines illustrate the tip temperature for fixed values of the power index parameter. i.e., for $\varepsilon_G = n = B = 0$, this suggests that the combined effect of power index parameters has no influence on heat transfer at all. The upper solid and dotted curves represent the maximum tip temperature corresponding to increased values of the power index parameter. i.e. for $\varepsilon_G = n = B = 0.5$ and middle two curves for intermediate values of power index parameter, i.e. for $\varepsilon_G = n = B = 0.25$. It is clear from the illustration that the combined influence of the power index parameter for the convective heat transfer coefficient, the internal heat generation sources, and the emissivity parameter of the fin surface collectively enhance the heat transfer process between the working fluids and the porous triangular fin. The higher value of ε_G, B and n imposes more nonlinearity in the energy equation and results higher tip temperature and escalate the rate of heat transfer. Along with the power law variation, a drop in tip temperature is also noted, with the increasing value of R_a form 0.001 to 0.1. When R_a increases, it raises the relative permeability of medium to penetrate more fluids which in turn contributes to increase of buoyant force in connection with the increase of power law parameters. The relative spacing between the solid and dotted line is more for $\varepsilon_G = n = B = 0.5$, which indicates that R_a is influences more heat transfer rate for higher value of power law parameters. **Figure 4** manifests the tip temperature of the triangular porous fin for three values of H_a at 0, 0.1

and 0.2 and each three values are separately analyzed when R_d at 0.001 and 0.1 respectively. The working fluids inside the porous fin are thought to be influenced by the external magnetic fields, which causes them to move more in order to transfer heat. Since H_a indicates the ratio of external magnetic field to the viscous force, the solid curve shows the tip temperature in the absence of an external magnetic field, indicating that the H_a has no effect on the fluid particles inside the fin. As the value of H_a increases, for greater mobility of the working fluids inside the fin, it increases the buoyancy force and reduces the viscous force. Consequently, the fluid particles convective heat transfer coefficient falls, strengthening the heat conduction process. The thermo physical parameter R_d indicates the combine mode of conduction and radiation from the base of the fin and it is evident that with an increasing the value of R_d, tip temperature increases for all values of H_a which implies that R_d influences the external magnetic effect of porous triangular fin. **Figure 5** describes variation of η, with respect value of Z_0 when power index parameters ε_G, n, B are equal to 0, 0.25 and 0.5 respectively. It has been observed that the fin efficiency is highest when power index parameters of q, ε and h is equal to 0 and increasing value of power index parameters, the fin efficiency decreases. Also the fin efficiency has decreasing trends with the increase of value Z_0. **Figure 6** describes the variation of η, with respect value to λ for values of R_a equal to 0.001 and 0.1 and effect of R_a are further exhibited when the values of ϕ is equal to 0.1 and 0.2 respectively. It is acceptable from the figure that, for higher value of ϕ, higher is the fin efficiency and also the efficiency curves has increased value when R_a is equal to 0.1. All the curves have an increasing trend with the increase of λ. **Figure 7** describes the variation of η, with respect value to ψ for the values of ε_G, n, B equal to 0, 0.25 and 0.5 while other parameters at fixed level. It has been found that the fin efficiency is highest when power index parameters of q, ε and h is equal to 0 and increasing value of power index parameters, the fin efficiency have decreasing trends with increase of ψ.

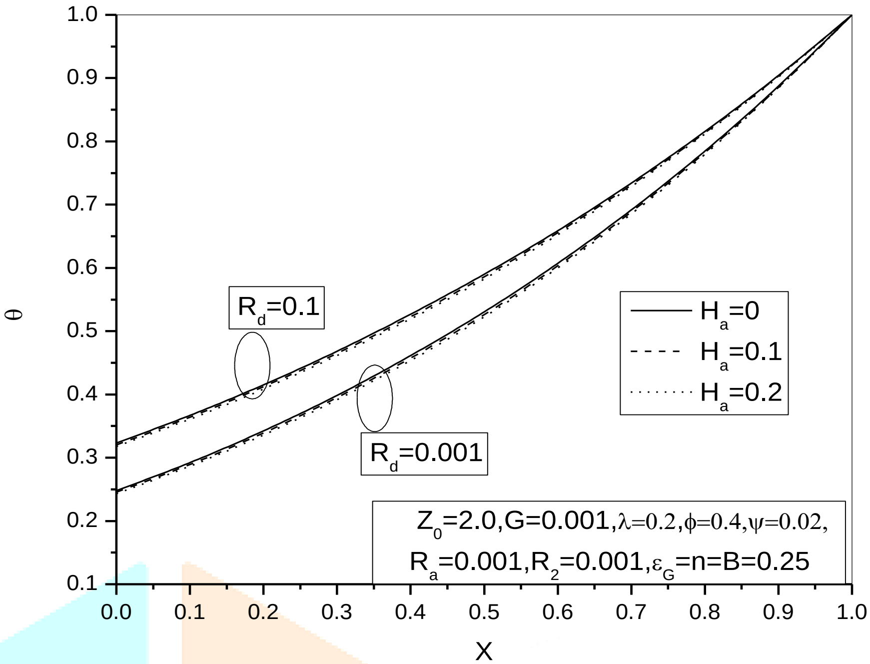

Figure 4. Effects of H_a on the temperature curves for the values of R_d at 0.001 and 0.1 respectively.

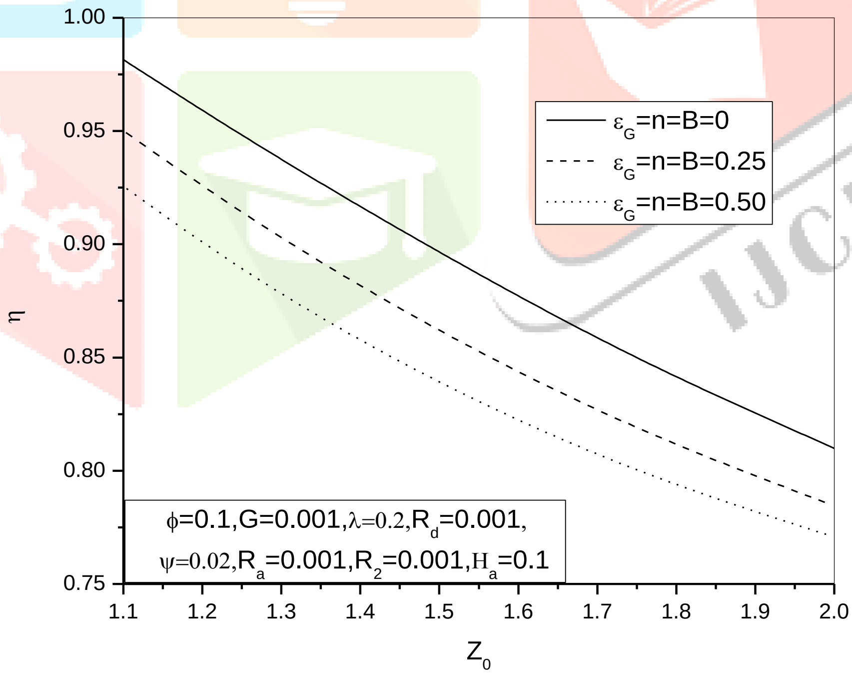

Figure 5. Effects of η with respect value of Z_0 for different values of power index parameters

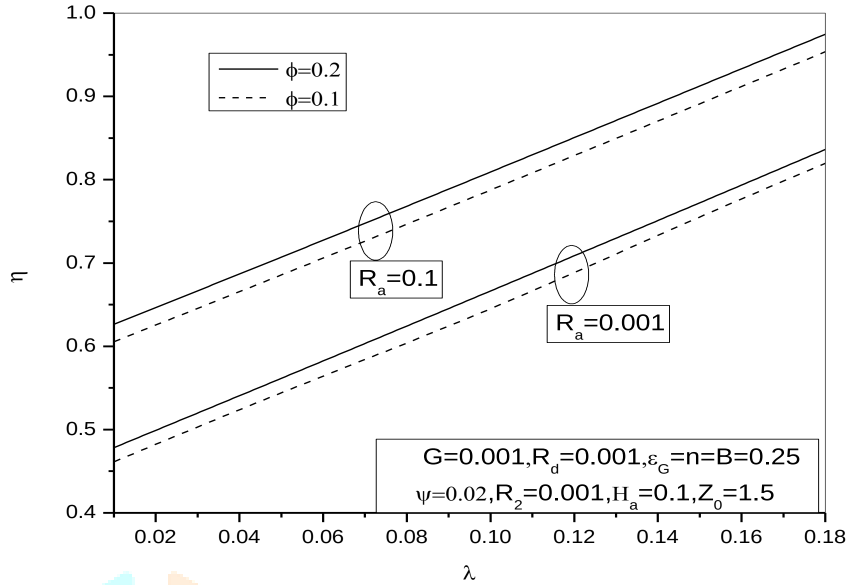

Figure 6. Effect of η with respect value to λ for values of R_a equal to 0.001 and 0.1 respectively.

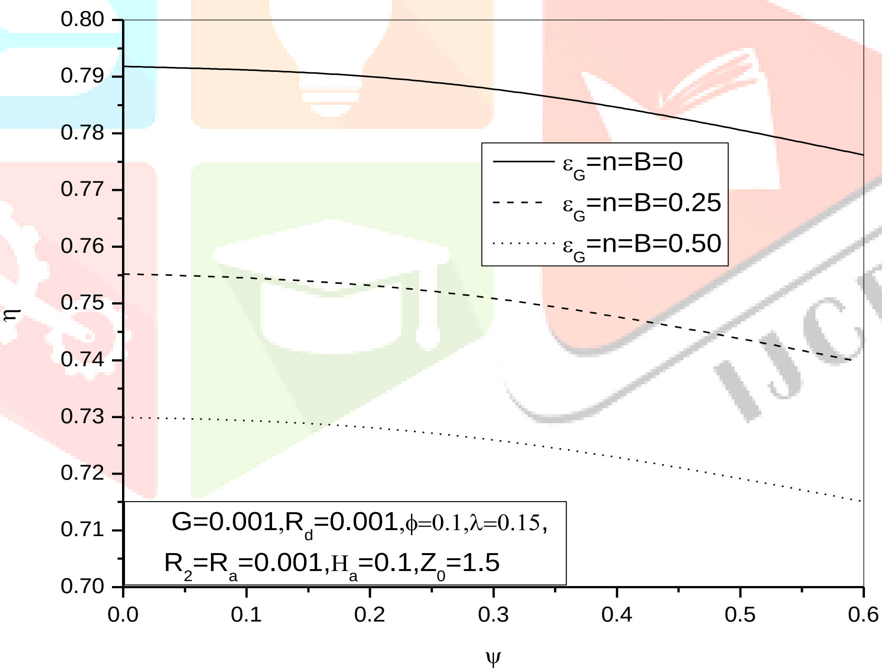

Figure 7. Effect of η with respect value to ψ for different values of power index parameters.

5. Conclusions

This study used the Modified Adomian Decomposition Method (MADM) to analyze the variation of power law-dependent heat transfer, internal heat generation, and surface emissivity in a triangular porous fin under external magnetic and electric fields. The results, compared with the Finite Difference Method (FDM), showed good agreement. It was found that increasing power law-dependent parameters raised the fin's tip temperature, enhancing heat transfer between the fluid and the fin.

The study found that increasing the Hartmann number, porosity, and base-to-width thickness improved fin efficiency, while wider fins had higher tip temperatures and heat transfer rates. Efficiency was highest when power law parameters were constant. MADM can also be applied to triangular or convex fins with varying thickness in future work.

References

[1] D Poulikakos, A Bejan. Fin geometry for minimum entropy generation in forced convection, Journal of Heat Transfer 104 (1982) 616-623. https://doi.org/10.1115/1.3245176.

[2] A. Shekarriz and OA Plumb. Enhancement of Film Condensation Using Porous Fins, Journal of Thermophysics and Heat Transfer, 3(3)1989) 309–314. https://doi.org/10.2514/3.28777.

[3] Kim SY, Paek JW, and Kang, BH. Flow and Heat Transfer Correlations for Porous Fin in a Plate-Fin Heat Exchanger, Journal of Heat Transfer 122 (3) (2000) 572–578. https://doi.org/10.1115/1.1287170

[4] Kem DQ, Kraus DA. Extended Surface Heat Transfer. McGraw–Hill, New York, 1972

[5] Vaszi AZ, Elliott L, Ingham DB and Pop I. Conjugate Free Convection from aVertical Plate Fin with a Rounded Tip Embedded in a Porous Medium, International Journal of Heat and Mass Transfer, 47(12–13) (2004) 2785–2794. https://doi.org/10.1016/j.ijheatmasstransfer.2004.01.001

[6] Kiwan S, and Zeitoun O. Natural Convection in a Horizontal Cylindrical Annulus Using Porous Fins, International Journal of Numerical Methods for Heat and Fluid Flow 18(5) (2008) 618–634. https://doi.org/10.1108/09615530810879747

[7] Kiwan S and Al-Nimr MA. Using Porous Fins for Heat Transfer Enhancement, Journal of Heat Transfer 123(4) (2001) 790–795. https://doi.org/10.1115/1.1371922.

[8] Kiwan S. Thermal analysis of natural convection in porous fins, Transport in porous media, 67(2006), 17–29. https://doi.org/10.1007/s11242-006-0010-3.

[9 Rama SR Gorla, AY Bakier. Thermal analysis of natural convection and radiation in porous fins, International Communications in Heat and Mass Transfer, 38(5) (2207) 638-645, https://doi.org/10.1016/j.icheatmasstransfer.2010.12.024.

[10] Balaram Kundu, Dipankar Bhanja, An analytical prediction for performance and optimum design analysis of porous fins, International Journal of Refrigeration 34 (2011) 337-352. https://doi.org/10.1016/j.ijrefrig.2010.06.011

[11] Balaram Kundu, Dipankar Bhanja, Thermal analysis of a construal T-shaped porous fin with radiation effects, International Journal of Refrigeration 34 (2011) 1483-1496. http://dx.doi.org/10.1016/j.ijrefrig.2011.04.003

[12] A Moradi,T Hayat, A Alsaedi, Convection-radiation thermal analysis of triangular porous fins with temperature dependent thermal conductivity by DTM, Energy Conversion and Management 77 (2014) 70-77. https://doi.org/10.1016/j.enconman.2013.09.016

[13] M Hatami, A Hasanpour, DD Ganji, Heat transfer study through porous fins (Si_3N_4 and AL) with temperature-dependent heat generation, Energy conversion and Management, 74 (2013) 9-16. https://doi.org/10.1016/j.enconman.2013.04.034

[14] Oguntala G, Sobamowo G, Abd-Alhameed, Stephen Jones, Efficient Iterative Method for Investigation of Convective–Radiative Porous Fin with Internal Heat Generation Under a Uniform Magnetic Field. International Journal of Applied Computation and Mathematics 5, 13 (2019), http://dx.doi.org/10.1007/s40819-022-01369-3

[15] Pranab Kanti Roy, Ashis Mallick, Hiranmoy Mondal, Sicelo Goqo, Precious Sibanda. Numerical study on rectangular-convex-triangular profiles with all variable thermal properties, International Journal of Mechanical Sciences 133, (2017): 251-259. https://doi.org/10.1016/j.ijmecsci.2017.07.066

[16] Pranab Kanti Roy, A decomposition solution of variable thickness absorber plate solar collectors with power law dependent thermal conductivity, Journal of Thermal Science and Engineering Applications14(8), (2022): 084501. https://doi.org/10.1115/1.4053118

[17] Soban Mosayebidorcheh, DD Ganji, Masud Farzinpoor, Approximate solution of the nonlinear heat transfer equation of a fin with power law temperature dependent thermal conductivity and heat transfer co-efficient, Propulsion and power Research, 3(1) (2014) :41-47. http://dx.doi.org/10.1016/j.jppr.2014.01.005

[18] Moitsheki RJ, Hayat T, and Malik MY. Some exact solutions of the fin problem with a power law temperature-dependent thermal conductivity, Nonlinear Analysis: Real World Applications, 11(5) 2010: 3287-3294. https://doi.org/10.1016/j.nonrwa.2009.11.021

[19] RJ Moitsheki, Steady one-dimensional heat flow in a longitudinal triangular and parabolic fin, Communication in Nonlinear Science and Numerical Simulations, 16, (2011): 3971-3980. https://doi.org/10.1016/j.cnsns.2011.01.010.

[20] MG Sobamowo, KC Alaribe, AO Adeleye, A Study on the Impact of Lorentz Force on the Thermal Behaviour of a Convective-Radiative Porous Fin using Differential Transformation Method, International Journal of Mechanical Dynamics & Analysis 6 (2020): 45-58.

[21] Das R, B Kundu, Predicting of heat generation and electromagnetic parameters from temperature response in porous fin, Journal of Thermo-physics and heat transfer 6 (2021): 45-58. http://dx.doi.org/10.2514/1.T6224

[22] Hoshyar HA, Ganji DD, Majidian AR. Least square method for porous fin in the presence of uniform magnetic field. J Appl Fluid Mech. 9(2) 2016: 661-668. https://doi.org/10.18869/acadpub.jafm.68.225.24245

[23] Patel T, Meher R. Thermal analysis of porous fin with uniform magnetic field using Adomian decomposition Sumudu transforms method. Nonlinear Eng. 6(3) (2017): 1-10. https://doi.org/10.1515/nleng-2017-0021.

[24] B. J. Gireesha, G. Sowmya, N. Srikantha. Heat transfer in a radial porous fin in the presence of magnetic field: a numerical study. International Journal of Ambient Energy 43(1) (2022): 3402-3409. https://doi.org/10.1080/01430750.2020.1831599.

[25] K. R. Madhura, Babitha, G. Kalpana, O. D. Makinde, Thermal performance of straight porous fin with variable thermal conductivity under magnetic field and radiation effects 49(8) 2020; 5002-2019. https://doi.org/10.1002/htj.21864.

[26] Das R, B Kundu. An estimate of heat generation, electric, and magnetic parameters from temperature fields in porous fins for electronic cooling system. IEEE Transactions on Components, Packaging and Manufacturing Technology 11(8) (2021): 1250 – 1257. 10.1109/TCPMT.2021.3099062.